

## Formation of soluble mercury oxide coatings: transformation of elemental mercury in soils

Miller, C. L., Watson, D. B., Lester, B., Howe, J. Y., Phillips, D. H., He, F., Liang, L., & Pierce, E. M. (2015). Formation of soluble mercury oxide coatings: transformation of elemental mercury in soils. *Environmental Science and Technology*, 49(20), 12105–12111. <https://doi.org/10.1021/acs.est.5b00263>

**Published in:**  
Environmental Science and Technology

**Document Version:**  
Peer reviewed version

**Queen's University Belfast - Research Portal:**  
[Link to publication record in Queen's University Belfast Research Portal](#)

### **Publisher rights**

This document is the Accepted Manuscript version of a Published Work that appeared in final form in *Environmental Science and Technology*, copyright 2015 © American Chemical Society after peer review and technical editing by the publisher.

To access the final edited and published work see <http://pubs.acs.org/doi/10.1021/acs.est.5b00263>

### **General rights**

Copyright for the publications made accessible via the Queen's University Belfast Research Portal is retained by the author(s) and / or other copyright owners and it is a condition of accessing these publications that users recognise and abide by the legal requirements associated with these rights.

### **Take down policy**

The Research Portal is Queen's institutional repository that provides access to Queen's research output. Every effort has been made to ensure that content in the Research Portal does not infringe any person's rights, or applicable UK laws. If you discover content in the Research Portal that you believe breaches copyright or violates any law, please contact [openaccess@qub.ac.uk](mailto:openaccess@qub.ac.uk).

## Article

**Formation of soluble mercury oxide coatings:  
transformation of elemental mercury in soils**Carrie L. Miller, David B. Watson, Brian Lester, Jane Y. Howe,  
Debra Helen Phillips, Feng He, Liyuan Liang, and Eric M. Pierce*Environ. Sci. Technol.*, **Just Accepted Manuscript** • DOI: 10.1021/acs.est.5b00263 • Publication Date (Web): 21 Sep 2015Downloaded from <http://pubs.acs.org> on September 22, 2015**Just Accepted**

"Just Accepted" manuscripts have been peer-reviewed and accepted for publication. They are posted online prior to technical editing, formatting for publication and author proofing. The American Chemical Society provides "Just Accepted" as a free service to the research community to expedite the dissemination of scientific material as soon as possible after acceptance. "Just Accepted" manuscripts appear in full in PDF format accompanied by an HTML abstract. "Just Accepted" manuscripts have been fully peer reviewed, but should not be considered the official version of record. They are accessible to all readers and citable by the Digital Object Identifier (DOI®). "Just Accepted" is an optional service offered to authors. Therefore, the "Just Accepted" Web site may not include all articles that will be published in the journal. After a manuscript is technically edited and formatted, it will be removed from the "Just Accepted" Web site and published as an ASAP article. Note that technical editing may introduce minor changes to the manuscript text and/or graphics which could affect content, and all legal disclaimers and ethical guidelines that apply to the journal pertain. ACS cannot be held responsible for errors or consequences arising from the use of information contained in these "Just Accepted" manuscripts.



ACS Publications

Title: Formation of soluble mercury oxide coatings: transformation of elemental mercury in soils

Carrie L. Miller\*<sup>a#</sup>, David B. Watson\*<sup>a</sup>, Brian P. Lester<sup>a</sup>, Jane Howe<sup>a,c</sup>, Debra H. Phillips<sup>b</sup>, Feng He<sup>a,d</sup>, Liyuan Liang<sup>a</sup>, Eric M. Pierce<sup>a</sup>

<sup>a</sup> Environmental Sciences Division, Oak Ridge National Laboratory, Oak Ridge, TN 37831, USA

<sup>#</sup> Troy University, Troy, AL 36082

<sup>b</sup> Queen's University Belfast, Belfast BT7 1NN, United Kingdom

<sup>c</sup> Hitachi High Technologies Canada, Inc., Toronto, ON

<sup>d</sup> College of Biological and Environmental Engineering, Zhejiang University of Technology, Hangzhou, Zhejiang 310032, China

\*Corresponding Author: Phone, (334) 670-3776; e-mail, [millerc@troy.edu](mailto:millerc@troy.edu) (C.L.M)

Phone,(865)241-4749; email, [watsondb@ornl.gov](mailto:watsondb@ornl.gov) (D. B.W)

Keywords: mercury, oxidation, soil

**Abstract**

The impact of mercury (Hg) on human and ecological health has been known for decades. Although a treaty signed in 2013 by 147 nations regulates future large-scale mercury emissions, legacy Hg contamination exists worldwide and small scale releases will continue. The fate of elemental mercury, Hg(0), lost to the subsurface and its potential chemical transformation that can lead to changes in speciation and mobility are poorly understood. Here we show that Hg(0) beads interact with soil or manganese oxide solids and x-ray spectroscopic analysis indicates that the soluble mercury coatings are HgO. Dissolution studies show that after reacting with a composite soil, > 20 times more Hg is released into water from the coated beads than from a pure liquid mercury bead. An even larger, > 700 times, release occurs from coated Hg(0) beads that have been reacted with manganese oxide, suggesting that manganese oxides are involved in the transformation of the Hg(0) beads and creation of the soluble mercury coatings. Although the coatings may inhibit Hg(0) evaporation, the high solubility of the coatings can enhance Hg(II) migration away from the Hg(0)-spill site and result in potential changes in mercury speciation in the soil and increased mercury mobility.

## 42 Introduction

43 More than 3000 mercury (Hg) contaminated sites exist worldwide due to the use of  
44 elemental Hg in industrial processes (chlor-alkali plants, artisanal and precious metal mining)  
45 and the conversion of mercury ore to elemental mercury in thermal processes (Hg mining and  
46 non-ferrous metal production). These Hg processing sites often contain soils contaminated with  
47 liquid elemental mercury ( $\text{Hg}(0)_l$ ).<sup>1</sup> Although a treaty signed in 2013 by 147 nations regulates  
48 future large-scale mercury emissions, legacy mercury contamination and small scale releases will  
49 continue to impact the environment.<sup>2</sup> Localized spills of  $\text{Hg}(0)_l$  can result in highly  
50 contaminated soils that are sources of Hg to the atmosphere and aquatic systems. The fate of  
51 elemental mercury lost to the subsurface and the potential for mercury release into groundwater  
52 and surface water remain poorly understood.

53 The speciation of Hg is dependent on both the source of Hg and the environment in  
54 which the Hg is deposited. The dominant Hg species in low level or uncontaminated soils  
55 include highly insoluble Hg-sulfide compounds such as metacinnabar (solubility =  $10^{-23.7}$  M) and  
56 potentially mobile Hg-organic complexes.<sup>3,4</sup>

57 Several methods, including sequential extractions, thermal analysis and Extended X-ray  
58 Absorption Fine Structure (EXAFS)<sup>5-13</sup> have been used to examine Hg speciation in Hg  
59 contaminated soils. Hg has been shown to be present in the form of  $\text{Hg}(0)_l$ , in addition to  
60 oxidized forms (e.g.,  $\text{Hg}(\text{II})$ ) associated with organics or mineral phases or as metacinnabar in  
61 contaminated sites.<sup>5-13</sup> In a study conducted with soils from the Amazon incubated with  $\text{Hg}(0)$ , it  
62 was determined using Hg thermal desorption methods, that 26-68% of the  $\text{Hg}(0)$  was converted  
63 to  $\text{Hg}(\text{II})$ .<sup>14</sup> Similarly using Hg thermal desorption analysis, 70-100% of the Hg adsorbed onto

platelets of various soil types and horizons were determined to have been transformed to oxidized Hg(II) after being saturated with Hg(0) vapors.<sup>15</sup> Although Hg-organic complexes typically dominate the speciation of mercury<sup>4, 12</sup> in uncontaminated soils, studies of soil contaminated with Hg(0)<sub>l</sub> have shown that Hg-sulfide species, such as metacinnabar, are more common<sup>3, 8, 13, 7</sup>. For example, at a site contaminated with Hg(0)<sub>l</sub> in Oak Ridge, TN, Hg in soils collected just below an accumulation of Hg(0)<sub>l</sub> was dominated by Hg-sulfide complexes. However, soil samples from the same site, which contained no Hg(0)<sub>l</sub> and had low Hg levels similar to uncontaminated sites, showed that the Hg was mostly present as Hg-organic complexes<sup>7</sup>. Hg-sulfide was also found in soils surrounding chlor-alkali facilities, where Hg(0)<sub>l</sub> spills occurred<sup>3, 13</sup>. The difference in Hg speciation in soils with and without Hg(0)<sub>l</sub> sources highlights the need to understand the chemical transformation of Hg(0)<sub>l</sub> in soils since these transformations will influence the mobility and speciation at Hg contaminated sites. Understanding these transformations is a critical step toward developing models to predict the movement of Hg at contaminated sites.

In a previous study we observed that Hg(0)<sub>l</sub> beads collected from contaminated Y-12 soils had a dull coatings on them<sup>7</sup>. In this study, we more closely examine the coatings on Hg(0)<sub>l</sub> beads that were removed from these soils. Laboratory experiments were conducted to examine changes in Hg speciation at the surface of Hg(0)<sub>l</sub> as a result of interaction with soils and pure mineral phases. We attempted to resolve the speciation of Hg on the surfaces of Hg(0)<sub>l</sub> beads using scanning electron microscopy. Changes in the solubility of mercury were evaluated in laboratory experiments using Hg(0)<sub>l</sub> before and after its interaction with soils and mineral phases. Collectively, the study aimed to examine transformation of the Hg(0)<sub>l</sub>.

## Experimental

### 87 *Soil collection*

88           Soil cores containing visible beads of liquid Hg were collected from the vadose zone in  
89 May 2011 from the Y-12 National Security Complex (Y-12) in areas with >1000 mg/kg Hg.<sup>7</sup> A  
90 dual-tube coring system was used to obtain cores to a depth of ~4.0 m. Soil and sediment were  
91 sampled from the cores at ~7.5-cm intervals and stored at 4° C until analysis.<sup>7</sup> Hg(0)<sub>l</sub> beads  
92 were carefully removed from the soil samples for laboratory experiments and SEM imaging,  
93 using a spatula to minimize any disturbance of the bead surfaces. An uncontaminated composite  
94 soil sample was prepared by combining soils from several locations at the Y-12 facility for use in  
95 laboratory experiments. Based on headspace analysis, these soil samples were found to be absent  
96 of Hg(0) vapors, so it was assumed they did not contain any Hg(0)<sub>l</sub>. After combining the soils,  
97 the composite was sieved through 2mm-sieve and homogenized by hand-mixing. The resultant  
98 composite had a total Hg concentration of 0.03 mg/kg. The concentration of other metals  
99 (Supporting Information Fig. S2) was determined, using an acid digestion followed by detection  
100 by inductively coupled plasma-mass spectrometry (EPA method 3050) for this composite  
101 sample.

### 103 *Imaging*

104           Scanning electron microscopy (SEM) and energy dispersive X-ray spectroscopy (EDS)  
105 were carried out using a Zeiss Merlin SEM equipped with a Bruker solid-state EDS detector and  
106 state-of-the-art in-lens detectors which enables high-resolution secondary imaging using low-  
107 energy electron beams. For SEM analysis, mercury beads were transferred to conductive carbon  
108 tape using tweezers. For large beads only a small portion of the bead and coating were extracted  
109 and used for analysis to minimize the amount of Hg(0) introduced into the SEM, since Hg(0)

vapors can amalgamate with parts of the SEM. A standard HgO powder obtained from Sigma Aldrich was used in SEM and EDS analysis for verification. The reagent grade Mn and Fe media used in the laboratory experiments were characterized by X-ray diffraction using a Panalytical Xpert diffractometer and X'Celerator detector. A search match was conducted using "Jade" (Materials Data, Inc.) and/or HighScore (PANalytical) software and the International Centre for diffraction data (ICDD) database to identify the solids. Details on the methods used for the SEM and EDS measurements are described in the Supporting Materials.

#### *Coating development on Hg(0)<sub>l</sub>*

Beads of Hg(0)<sub>l</sub> were exposed to a range of media (Table 1) to examine factors controlling the formation of the coating on the bead surface under controlled experimental conditions. For laboratory experiments Hg(0)<sub>l</sub> (Fisher, Laboratory grade) was washed with nitric acid (1.4 M) followed by three rinses with deionized water (18.2 megohm). Washed Hg(0)<sub>l</sub> was stored in a vial containing deoxygenated water with a N<sub>2</sub> gas filled headspace as a 'stock Hg(0)<sub>l</sub>'. For dissolution experiments small beads of washed Hg(0)<sub>l</sub> (50 µl) were removed from the stock container using a gas tight syringe in a N<sub>2</sub> gas filled glove bag and placed in 5 ml glass vials. The solid phase media was added to the vial so that the bead was completely covered by the fine granular solid being tested. The beads of Hg(0)<sub>l</sub> were allowed to react in the dark, without agitation, with the solid for 8-157 days. At the end of the treatment, beads were recovered using a spatula and placed in 40 mL amber glass vials for aqueous dissolution studies (see next section). Laboratory tests were conducted under oxic ambient atmospheric conditions unless noted. Control experiments, using the pure stock Hg(0)<sub>l</sub>, were performed and used as a baseline to compare to all other treatments. Solid media, including Fe<sub>2</sub>O<sub>3</sub>, MnO<sub>2</sub> and Mn<sub>2</sub>O<sub>3</sub>, clay and



quartz were characterized before use (see Supporting Information). For all experiments, except when noted, the solids were used as received – no attempt was made to remove moisture. To determine the effect of free water on  $\text{Hg}(0)_l$  transformation by solid media, oven dried ( $105^\circ\text{C}$ )  $\text{Mn}_2\text{O}_3$  samples were used and results were compared to the other treatments. After oven drying, the  $\text{Mn}_2\text{O}_3$  sample was held in a  $\text{N}_2$  flushed glove bag containing a calcium sulfate desiccant.

The presence of oxidized Hg associated with the  $\text{Hg}(0)_l$  beads was determined by measuring the dissolved  $\text{Hg}(\text{II})$  after the addition of water to the bead. Deionized water was added to the glass vial containing treated beads and the vial was immediately capped. The vial cap was fitted with an outlet port consisting of Teflon tube (1.6 mm internal diameter) secured approximately 10 mm from the base of the vial (Supporting Information Fig. S3). Aqueous samples (1 ml) were withdrawn from the vial with a plastic syringe following a 0.5 mL flush of the sample line. A sub-sample was immediately analyzed for dissolved  $\text{Hg}(0)_{\text{aq}}$  and the remaining aliquot was preserved with bromine monochloride ( $\text{BrCl}$ ) for total mercury analysis. A 20 ml syringe filled with air was used to equilibrate the headspace of the vial as the liquid sample was removed. The contents in the glass vials were gently mixed using a rotating table (160 rpm) during the course of the experiment. The concentrations of dissolved  $\text{Hg}(0)_{\text{aq}}$  and total Hg were measured multiple times between 10 and 300 minutes using a modification<sup>7</sup> of EPA method 1631E. For  $\text{Hg}(0)_{\text{aq}}$  measurements, the  $\text{Hg}(0)$  was purged from the sample (50  $\mu\text{l}$  sample added to  $\sim 10$  mL of mercury free water) and detected using cold vapor atomic absorption spectroscopy (CVAAS; RA-915+Hg, Ohio Lumex). For total Hg analysis, the samples were treated with  $\text{BrCl}$  for a minimum of 24 hours to oxidize the  $\text{Hg}(0)$  and organic matter in the sample. Stannous chloride was added to the sample and the resulting  $\text{Hg}(0)$  was purged and detected using CVAAS. Analytical detection limits were calculated daily and the

values were always below 100 pg. All samples, with the exception of the blanks, were above this detection limit. The average standard deviation between duplicate HgT measurements were 1.5% and the average recovery of routinely analyzed reference materials (IAEA433, NIST 8407 and CRM 580) was 98(+/-3)%. Analytical blanks and procedural blanks, which quantified the Hg associated with the experimental containers, were below detection limits. The concentration of Hg(II) was determined as the difference between the total Hg and dissolved Hg(0) concentration. Concentrations of Hg(II) released from the beads were normalized to the bead surface area, determined from the bead volume or weight and the density of mercury, assuming a spherical bead. This normalization was conducted to adjust for the different sizes of beads removed from Hg(0) contaminated soils.

## Results and Discussion

### *Hg coatings on Hg(0)<sub>l</sub> beads*

Transformations of Hg(0)<sub>l</sub> in soils were examined by using samples collected at the Y-12 facility, which are contaminated due to Hg(0)<sub>l</sub> use and multiple spills between 1950-1963<sup>7, 16</sup>. Mercury beads from the mercury spill site are clearly shown in photograph (Fig. 1a) ranging from microscopic to mm sizes. Compared to a clean, pure Hg(0)<sub>l</sub> (Fig. 1b), a dull coating is clearly seen on beads in the soils. Closer examination with SEM (Fig. 1e) of a Hg(0)<sub>l</sub> bead from the contaminated soil shows a distinct solid phase coating. The dull coatings were also observed with Hg(0)<sub>l</sub> beads that had been reacted with soils in the laboratory (Fig. 1 c,d). Microstructural analysis of Hg(0)<sub>l</sub> of a bead extracted from the Y-12 soil cores revealed ubiquitous clusters of crystals on the surface (Fig. 2a-b). Comparing EDS analyses of crystals on the exterior of the bead and the Hg(0)<sub>l</sub> on the interior of the bead indicates that the crystalline solid is a mercury

oxide (Fig. 2c). EDS spectra (Fig. 2d) collected from both a solid crystal and liquid interior spot of the bead (Fig. 2c) show that both regions contain a peak at approximately 2.2 keV, which is indicative of the Hg. However, the EDS spectrum of the solid crystal also contains a strong peak at 0.5 keV, corresponding to the presence of oxygen in the structure of the crystals, which agreed well with the EDS spectra of the standard HgO (Supporting Information Fig. S4b). The crystals in the SEM images (Fig 2a-c) have an orthorhombic structure that also resembles the structure of the HgO montroydite (Supporting Information Fig. S4a). The crystals from this sample ranged from 10 to 1000 nm in size. Clay particles were also observed on the surface of the beads (Fig. 2a).

Laboratory experiments demonstrate that when placed in deionized water,  $\text{Hg}(0)_\text{l}$  beads extracted from the Y-12 soils [in-situ  $\text{Hg}(0)_\text{l}$ ] release oxidized Hg at concentrations 15-45 times greater than pure beads of  $\text{Hg}(0)_\text{l}$  (Fig. 3). The oxidized Hg is in either the +1 or +2 valance state; hereafter,  $\text{Hg}(\text{II})$  is used to signify both Hg oxidation states because the analytical methods do not distinguish between the two and  $\text{Hg}(\text{II})$  is the inorganic mercury form typically found in the environment. For pure, stock  $\text{Hg}(0)_\text{l}$  beads, the amount of  $\text{Hg}(\text{II})$  released, based on bead surface area, at initial (~10 minutes) and final (300 minutes) time points, was  $1.7 (\pm 0.9)$  and  $7.6 (\pm 4.0)$   $\text{nmol}/\text{m}^2$ , respectively. This gradual increase over time is in part due to the oxidation of dissolved gaseous mercury ( $\text{Hg}(0)_\text{d}$ ) and is consistent with other studies<sup>17</sup>. Two  $\text{Hg}(0)_\text{l}$  beads from contaminated soil (with mass of 0.974 g and 0.588g) respectively released  $\text{Hg}(\text{II})$  at 61.4  $\text{nmol}/\text{m}^2$  and 30.8  $\text{nmol}/\text{m}^2$  within the first 10 minutes, under the same experimental conditions used for the pure  $\text{Hg}(0)_\text{l}$  beads (Fig. 3). Such rapid release of  $\text{Hg}(\text{II})$  suggests that oxidized Hg species are present on the surface of the  $\text{Hg}(0)_\text{l}$  beads collected from *in situ* soils and are rapidly dissolved in water (Supporting Information Fig. S1, Discussion 1). This is consistent with the

spectroscopic characterization where SEM and EDS suggested the presence of HgO on the surface of Hg(0)<sub>l</sub> beads associated with contaminated site soil.

#### *Oxidation of Hg(0)<sub>l</sub> by solid phase media*

Subsequent laboratory experiments were conducted to determine which common mineral assemblages found in soil result in the same oxidation of Hg, and formation of coatings on the surface of Hg(0)<sub>l</sub> beads, that is observed in Y-12 soils. To varying degrees we observed the oxidation of the Hg(0) and coating formation using pure Hg(0)<sub>l</sub> beads, covered by an uncontaminated soil composite from Y-12 and a few other solid media, including Fe and Mn oxides, kaolinite, and silica sand (Table 1, Fig. 4). In this set of experiments, pure stock Hg(0)<sub>l</sub> beads were reacted with various solid phases for set time periods in an ambient laboratory atmosphere. Ambient laboratory air was routinely measured and the Hg concentrations were below detection limits. After reaction periods, the beads were removed from the solid media and dissolution experiments were conducted to determine the amounts of Hg(II) released to water. After pure Hg(0)<sub>l</sub> was covered by the clean composite soil for 10 days, the Hg(II) released was 14 times greater than from a pure bead not exposed to a solid. Similar results were obtained when Hg(0)<sub>l</sub> was added to the soil composite that was held in a nitrogen filled anaerobic glove bag prior to the incubation to remove oxygen (Fig. 4), suggesting oxygen is not essential for oxidation of the Hg(0)<sub>l</sub>. The amounts of Hg(II) released from Hg(0)<sub>l</sub> beads reacted with the soil composite for 10, 30 and 157 days, were similar to the Hg(II) released from the Hg(0)<sub>l</sub> beads removed from the contaminated Y-12 soils.

Reaction of manganese oxides (MnO<sub>2</sub> and Mn<sub>2</sub>O<sub>3</sub>) with pure Hg(0)<sub>l</sub> beads enhanced Hg(II) release into water by amounts similar to or greater than observed for Hg(0)<sub>l</sub> recovered

from contaminated Y-12 soil (Fig 4). Eight day reactions of  $\text{Hg}(0)_l$  with  $\text{MnO}_2$  resulted in the same order of magnitude increased release of  $\text{Hg}(\text{II})$  as the in-situ  $\text{Hg}(0)_l$  beads. Reaction of  $\text{Hg}(0)_l$  beads with  $\text{Mn}_2\text{O}_3$  for 10 and 120 days significantly increased  $\text{Hg}(\text{II})$  releases into water, at concentrations of 89 and 741 times greater than for pure  $\text{Hg}(0)_l$  beads, respectively. An increase in soluble  $\text{Hg}(\text{II})$  in water was also found when  $\text{Hg}(0)_l$  was reacted with sand, kaolinite and  $\text{Fe}_2\text{O}_3$ ; but these increases, were only 2-3 fold greater than for pure  $\text{Hg}(0)_l$  and less than either the in-situ  $\text{Hg}(0)_l$  beads or the Mn oxide treated  $\text{Hg}(0)_l$  beads. We hypothesize that minor amounts of impurities (e.g., Mn oxides) in the sand,  $\text{Fe}_2\text{O}_3$  and other solids, account for the surface oxidation of  $\text{Hg}(0)_l$  beads that leads to  $\text{Hg}(\text{II})$  dissolution in water. It is also possible that these silica sand related solid have the ability to oxidize  $\text{Hg}(0)_l$  but this oxidation is much less than observed with Mn minerals. It is also less than observed with soils so it is unlikely that these sand related solids are significantly influencing the oxidation of  $\text{Hg}(0)_l$  under natural condition.

In a recent study, the conversion rate of  $\text{Hg}(0)$  incubated in Amazon soils to  $\text{Hg}(\text{II})$  was determined to be 36-88% by thermal desorption analysis, and was correlated to the presence of Mn.<sup>47</sup> It was hypothesized that Mn is one of the major species responsible for the Hg-oxidation process but that more detailed studies are required to clarify this effect.<sup>47</sup> At another gold mining site in South America, known for spills of  $\text{Hg}(0)$ , the only form of Hg found based on thermal desorption analysis was  $\text{Hg}(\text{II})$  and was also correlated to the presence of Mn.<sup>48</sup> Mn(IV) and Mn(III) oxides are capable of oxidizing metal ions including arsenic (III), cobalt (II), uranium (IV) and chromium (III) in water,<sup>18-27</sup> but redox interactions with  $\text{Hg}(0)_l$  in soils have not been reported. In natural systems, Mn oxides exist in +2, +3, and +4 oxidation states, and are ubiquitous in soils and sediments worldwide<sup>24</sup>. Reported Mn oxide concentrations in soil on the

Oak Ridge Reservation, where we collected  $\text{Hg}(0)_l$  contaminated soils for our study, were up to 0.8% by weight.<sup>28</sup>

Since most soils contain some moisture, we also examined the potential involvement of free water in the oxidation of  $\text{Hg}(0)_l$  by Mn oxides. Coated  $\text{Hg}(0)_l$  beads were prepared using air dried  $\text{Mn}_2\text{O}_3$ , which likely contained trace amounts of free water, and also with  $\text{Mn}_2\text{O}_3$  that had been oven dried at 105°C and held in a  $\text{N}_2$  flushed glove bag containing a desiccant. The amounts of  $\text{Hg}(\text{II})$  released in water after 10-day treatments from the two procedures were similar (Fig. 4) and suggests that the presence of free water may not control the oxidized coatings on the  $\text{Hg}(0)_l$  beads. The oven drying of the  $\text{Mn}_2\text{O}_3$  is not expected to remove all mineral bound water, so the possibility of bound water in facilitating the oxidation of  $\text{Hg}(0)_l$  needs to be further studied.

The mechanism controlling the solid phase oxidation of  $\text{Hg}(0)_l$  is not completely understood. In other studies that have examined  $\text{Hg}(0)$  oxidation under aqueous conditions<sup>18, 29-31</sup>, the oxidation of dissolved gaseous Hg is slow unless a liquid  $\text{Hg}(0)$  metal droplet is present<sup>18</sup>. The oxidation rate increases in the presence of ligands such as chloride or thiols and the reaction appears to occur at the surface of the  $\text{Hg}(0)_l$  bead<sup>18, 29</sup>. Increasing the oxygen concentration in the solution resulted in an increase in  $\text{Hg}(0)$  oxidation, suggesting that oxygen is required for this aqueous reaction<sup>18</sup>. In our solid phase oxidation experiments, no change in the subsequent release of  $\text{Hg}(\text{II})$  was found, irrespective of whether the treatment was performed in a  $\text{N}_2$  or  $\text{O}_2$  atmosphere. However,  $\text{Hg}(0)_l$  oxidation by dissolved oxygen was observed in the presence of sediment and water<sup>31</sup>. In that study, because the oxidation at the surface of  $\text{Hg}(0)_l$  was not specifically examined – in the presence of water and sediment, it cannot be determined if the  $\text{Hg}(0)_l$  or dissolved  $\text{Hg}(0)$  was oxidized in the experiments.

The oxidation of Hg(0) in the gas phase has been extensively studied, since this process is used to create Hg(II) in the flue gases of coal fired power plants to reduce atmospheric Hg emissions<sup>32</sup>. Mn oxides have been examined as catalysts for Hg(0) oxidation in the gas phase<sup>33-35</sup>. In this process, the Mn oxide reacts with HCl in the flue gas and the activated chlorine species acts as the oxidant for the Hg(0)<sup>36</sup>. Oxidation of Hg(0) in the atmosphere<sup>37</sup> and in surface waters is believed to be primarily photochemically driven<sup>38-39</sup> and therefore is quite different from our study, where the solid phase reaction of Hg(0) occurred in dark soils with limited exposure to light.

Although Mn oxides have been shown to oxidize metal ions such as arsenic, cobalt, uranium and chromium<sup>19-27</sup> in solution, oxidation of liquid Hg(0)<sub>l</sub> in soils by Mn oxides has not been reported. For other metals the oxidation occurs under aqueous conditions and the water is an important component in the reaction. The reaction of Hg(0)<sub>l</sub> we observed with solid mineral phases did not involve free water, and the involvement of water is only through the trace amounts bound to the mineral surfaces. In the absence of detailed study we could only speculate that oxidation of Hg(0)<sub>l</sub> may be initiated by the formation of an amalgam between Hg and Mn<sup>40</sup> followed by Hg(0)<sub>l</sub> reduction of Mn<sup>2+</sup> species (this is used to analyze Mn by mercury hanging-drop electrodes)<sup>41</sup>. The formation of Hg amalgam in soil, followed by electron transfer from Hg(0) to Mn(III/IV), is a feasible mechanism for the formation of the HgO coatings in soils. Additional work is required to understand the mechanism of Hg(0)<sub>l</sub> oxidation in soils.

## Environmental Implications

Our studies aimed to understand how  $\text{Hg}(0)_\text{l}$  beads are transformed in ambient soils and mineral assemblages, by investigating the solid phase oxidation of  $\text{Hg}(0)_\text{l}$  and is the first to observe the formation of  $\text{HgO}$  crystals on the surface of  $\text{Hg}(0)$  bead. Biester and coauthors<sup>42</sup> noted that  $\text{Hg}$  species in soils surrounding a mercury mine were released from the soil at temperatures expected for the release of  $\text{HgO}$ . They inferred that  $\text{HgO}$  formed during heating of  $\text{Hg}$ -containing ores to recover  $\text{Hg}$  from the mined material based on the assumption that the  $\text{HgO}$  only formed at temperatures between 300-350°C. Similarly, asymmetric particles of  $\text{Hg}$  were found after soil containing  $\text{Hg}(0)_\text{l}$  from a chlor-alkali plant was thermally treated at 220°C<sup>43</sup> and it was suggested that  $\text{HgO}$  or  $\text{HgSO}_4$  formed due to the thermal treatment. In our study, the  $\text{Hg}(0)_\text{l}$  beads have been in contact with the soil for decades following their spills at the site. The  $\text{HgO}$  crystallites present on these beads would have been formed at ambient temperature, because the elevated temperatures noted by others, did not exist in surface soils. The presence of  $\text{HgO}$  in  $\text{Hg}(0)_\text{l}$  contaminated soils indicates that the formation of  $\text{HgO}$  as patchy crystals or coatings on  $\text{Hg}(0)_\text{l}$  beads likely occurs at  $\text{Hg}(0)_\text{l}$  contaminated sites worldwide.

The formation of  $\text{HgO}$  on  $\text{Hg}(0)_\text{l}$  could increase  $\text{Hg}$  mobility since  $\text{HgO}$ , with a solubility of  $10^{-3.6} \text{ M}$ <sup>44,45</sup>, is 3 orders of magnitude more soluble than  $\text{Hg}(0)$  and has a high rate of dissolution ( $\sim 10^{-9} \text{ mol cm}^{-2} \text{ s}^{-1}$ )<sup>44</sup>. The observation of  $\text{HgO}$  crystallites on  $\text{Hg}(0)_\text{l}$  does not imply that  $\text{HgO}$  will be a dominate form of mercury at sites contaminated with  $\text{Hg}(0)_\text{l}$ . As  $\text{HgO}$  dissolves in water,  $\text{Hg(II)}$  would form strong complexes with reduced sulfur, organic matter, and surface functional groups of minerals such as iron oxyhydroxides and Mn oxides.<sup>3,4,7-9, 12, 46-48</sup> It is thus expected that the  $\text{HgO}$  formed at the surface of the  $\text{Hg}(0)_\text{l}$  will continue to change, and the lifespan of  $\text{HgO}$  in soil will depend on the hydrologic conditions in the soil. Whereas the porewater movement will control the solubilization and mobility of the  $\text{HgO}$  at the bead surface,



the composition of the surrounding soils will determine the types of Hg(II) complexes and persistence of Hg in soils. Transformation of the HgO is expected to occur in ground and/or surface waters, since HgO is thermodynamically unstable under most environmental conditions, and the kinetics of the transformation requires further investigation.

A recent study of 3000 mercury contaminated sites worldwide estimated Hg release at a rate of 116 Mg yr<sup>-1</sup> from contaminated sites into the hydrosphere. Chlor-alkali facilities, with over 150 active and inactive sites identified globally, have historic contamination of Hg(0)<sub>l</sub> in soils and sediments, and more than 40% of these facilities are estimated to be located adjacent to coastal or riverine systems<sup>1</sup>. At the Y-12 complex in Oak Ridge, TN it is estimated that approximately 193,000 kg of Hg was lost to the environment and ~6.7 kg Hg leaves the site annually via surface water discharges alone and the Hg is primarily in the form of dissolved oxidized Hg(II).<sup>16</sup> The flux of dissolved Hg(II) is likely impacted by the HgO coating we observe on the ubiquitous Hg(0)<sub>l</sub> found at the site. Rainfall, water flow, and HgO dissolution processes in combination would influence Hg(II) transport in water. High concentrations of Hg(II) have also been observed in streams associated with artisanal gold mining operations that use Hg(0)<sub>l</sub>. At a site in Indonesia, where highly contaminated Hg wastes were disposed of, total Hg was detected in surface water at concentrations as high as 9.1 ug/L and 95% was determined to be Hg(II)<sup>46</sup>. The increased mobility of Hg associated with the formation of oxidized Hg coatings will be especially important in environments where hydrologic cycles create conditions for the formation of HgO during dry periods and mobilization during wet periods.

Hg(0)<sub>l</sub> contaminated sites resulting from artisanal gold mining and industrial processes are present as long term sources of Hg to the environment.<sup>1</sup> Our study shows that the formation and dissolution of HgO coatings have the potential for enhanced migration of Hg(II). Our

laboratory study indicates that up to 700 times more Hg(II) may be released from Hg beads with coating than without. Thus this potentially important phenomenon needs to be considered when assessing the long-term fate of mercury at these sites. The rate at which Hg distributes through the water environment may be greatly underestimated if the formation of soluble HgO coatings is not taken into consideration.

### Author Contributions

C.L.M. and D.B.W contributed equally to this work.

### Acknowledgements

The authors would like to thank Kenneth Lowe for field sampling assistance and Stephen Field and Terry Cothron of B&W Y-12 for assistance in coordinating the collection of field samples at the Y-12 facility. Roberta Ann Meisner of ORNL conducted the XRD analyses. This research was supported by the Office of Groundwater and Soil Remediation, Office of Environmental Management, US Department of Energy (DOE) as part of the Applied Field Research Initiative Program at Oak Ridge National Laboratory (ORNL), which is managed by UT-Battelle LLC for the US DOE under Contract No. DE-AC05-00OR22725. The SEM work was in part sponsored by ORNL's Shared Research Equipment (ShaRE) User Program, which is sponsored by the Office of Basic Energy Sciences, US DOE. This manuscript has been authored by UT-Battelle, LLC under Contract No. DE-AC05-00OR22725 with the US Department of Energy. The United States Government retains and the publisher, by accepting the article for publication, acknowledges that the United States Government retains a non-exclusive, paid-up, irrevocable, world-wide license

to publish or reproduce the published form of this manuscript, or allow others to do so, for United States Government purposes. The Department of Energy will provide public access to these results of federally sponsored research in accordance with the DOE Public Access Plan (<http://energy.gov/downloads/doe-public-access-plan>).

## Supporting Information Available

This information is available free of charge via the Internet at <http://pubs.acs.org>

## References

1. Kocman, D.; Horvat, M.; Pirrone, N.; Cinnirella, S. Contribution of contaminated sites to the global mercury budget. *Environ. Res.* **2013**, 125, 160-170.
2. Krabbenhoft, D. P.; Sunderland, E. M. Global change and mercury. *Science* **2013** 341, 1457-1458.
3. Bloom, N. S.; Preus, E.; Katon, J.; Hiltner, M. Selective extractions to assess the biogeochemically relevant fractionation of inorganic mercury in sediments and soils. *Anal. Chim. Acta.* **2003** 479, 233-248.
4. Skjellberg, U. Competition among thiols and inorganic sulfides and polysulfides for Hg and MeHg in wetland soils and sediments under suboxic conditions: Illumination of controversies and implications for MeHg net production. *J. Geophys. Res. [Biogeoscience]*, **2008**, 113, G00C03.
5. Biester, H.; Nehrke, G. Quantification of mercury in soils and sediments - Acid digestion versus pyrolysis. *Fresen J Anal Chem.* **1997**, 358, 446-452.
6. Bollen, A.; Wenke, A.; Biester, H. Mercury speciation analyses in HgCl<sub>2</sub>-contaminated soils and groundwater - Implications for risk assessment and remediation strategies. *Water Res.* **2008**, 42, 91-100.
7. Miller, C. L.; Watson, D. B.; Lester, B. P.; Lowe, K. A.; Pierce, E. M.; Liang, L. Characterization of soils from an industrial complex contaminated with elemental mercury *Environ. Res.* **2013**, 125, 20-29.
8. Kocman, D.; Horvat, M.; Kotnik, J. Mercury fractionation in contaminated soils from the Idrija mercury mine region. *J. Environ. Monit.* **2004**, 6, 696-703.
9. Kim, C.; Bloom, N.; Rytuba, J.; Brown, G. 2003. Mercury speciation by X-ray absorption fine structure spectroscopy and sequential chemical extractions: a comparison of speciation methods. *Environ. Sci. Technol.* **2003**, 37, 5102-5108.
10. Kim, C.; Rytuba, J.; Brown, G. Geological and anthropogenic factors influencing mercury speciation in mine wastes: an EXAFS spectroscopy study. *Appl. Geochem.* **2004**, 19, 379-393.

11. Skyllberg, U.; Bloom, P.; Qian, J.; Lin, C.; Bleam, W.F. Complexation of mercury(II) in soil organic matter: EXAFS evidence for linear two-coordination with reduced sulfur groups. *Environ. Sci. Technol.* **2006** *40*, 4174–4180.
12. Guedron, S.; Grangeon, S.; Lanson, B.; Grimaldi, M. Mercury speciation in a tropical soil association; Consequence of gold mining on Hg distribution in French Guiana. *Geoderma* **2009**, *153*, 331–346.
13. Neculita, C.; Zagury, G.; Deschenes, L. Mercury speciation in highly contaminated soils from chlor-alkali plants using chemical extractions. *J. Environ. Qual.* **2005**, *34*, 255–262.
14. Valle, C. M.; Santana, G. P.; Windmüller, C. C. Mercury conversion processes in Amazon soils evaluated by thermodesorption analysis. *Chemosphere* **2006**, *65*, 1966–1975.
15. Soares, Liliane Catone; Egreja Filho, Fernando Barboza; Linhares, Lucília Alves; Windmoller, Cláudia Carvalhinho; Yoshida, Maria Irene. Accumulation and oxidation of elemental mercury in tropical soils. *Chemosphere* **2015**, *134*, 181–191.
16. Brooks, S. C.; Southworth, G. R. History of mercury use and environmental contamination at the Oak Ridge Y-12 Plant. *Environ. Pollut.* **2011**, *159*, 219–228.
17. Amyot, M.; Morel, F. M. M.; Ariya, P. A. Dark oxidation of dissolved and liquid elemental mercury in aquatic environments. *Environ. Sci. Technol.* **2005**, *39*, 110–114.
18. Chiu, V. Q.; Hering, J. G. Arsenic adsorption and oxidation at manganite surfaces. 1. Method for simultaneous determination of adsorbed and dissolved arsenic species. *Environ. Sci. Technol.* **2000**, *34*, 2029–2034.
19. Fendorf, S. E.; Zasoski, R. J. Chromium (III) oxidation by delta-MnO<sub>2</sub> 1. Characterization. *Environ. Sci. Technol.* **1992**, *26*, 79–85.
20. Kim, J. G.; Dixon, J. B.; Chusuei, C. C.; Deng, Y. J. Oxidation of chromium(III) to (VI) by manganese oxides. *Soil Sci. Soc. Am. J.* **2002**, *66*, 306–315.
21. Kozuh, N.; Stupar, J.; Gorenc, B. Reduction and oxidation processes of chromium in soils. *Environ. Sci. Technol.* **2000**, *34*, 112–119.
22. Manceau, A.; Drits, V. A.; Silvester, E.; Bartoli, C.; Lanson, B. Structural mechanism of Co<sup>2+</sup> oxidation by the phyllomanganate buserite. *Am. Mineral.* **1997**, *82*, 1150–1175.
23. Oscarson, D. W.; Huang, P. M.; Defosse, C.; Herbillon, A. Oxidative power of Mn(IV) and Fe(III) oxides with respect to As(III) in terrestrial and aquatic environments. *Nature* **1981**, *291*, 50–51.
24. Post, J. E. Manganese oxide minerals: Crystal structures and economic and environmental significance. *Proc. Natl. Acad. Sci. U. S. A.* **1999**, *96*, 3447–3454.
25. Risser, J. A.; Bailey, G. W. Spectroscopic study of surface redox reaction with manganese oxides. *Soil Sci. Soc. Am. J.* **1992**, *56*, 82–88.
26. Stepniewska, Z.; Bucior, K.; Bennicelli, R. P. The effects of MnO<sub>2</sub> on sorption and oxidation of Cr(III) by soils. *Geoderma* **2004**, *122*, 291–296.
27. Wang, Z. M.; Lee, S. W.; Kapoor, P.; Tebo, B. M.; Giammar, D. E. Uraninite oxidation and dissolution induced by manganese oxide: A redox reaction between two insoluble minerals. *Geochim. Cosmochim. Acta* **2013**, *100*, 24–40.
28. Phillips, D. H.; Watson, D. B.; Roh, Y. Uranium deposition in a weathered fractured Saprolite/Shale. *Environ. Sci. Technol.* **2007**, *41*, 7653–7660.
29. Yamamoto, M. Possible mechanism of elemental mercury oxidation in the presence of SH compounds in aqueous-solution. *Chemosphere* **1995**, *31*, 2791–2798.

30. Yamamoto, M. Stimulation of elemental mercury oxidation in the presence of chloride ion in aquatic environments. *Chemosphere*. **1996**, 42, 1217-1224.
31. Dominique, Y.; Muresan, B.; Duran, R.; Richard, S.; Boudou, A. Simulation of the chemical fate and bioavailability of liquid elemental mercury drops from gold mining in Amazonian freshwater systems. *Environ. Sci. Technol.* **2007**, 41, 7322-7329.
32. Wilcox, J.; Rupp, E.; Ling, S.; Lim, D.; Negreira, A.; Kirchofer, A.; Feng, F.; Lee, K. Mercury adsorption and oxidation in coal combustion and gasification processes. *Int. J. Coal Geol.* **2012**, 90, 4-20.
33. Li, J.; Yan, N.; Qu, Z.; Qiao, S.; Yang, S.; Guo, Y.; Liu, P.; Jia, J. Catalytic Oxidation of Elemental Mercury over the Modified Catalyst Mn/ $\alpha$ -Al<sub>2</sub>O<sub>3</sub> at Lower Temperatures. *Environ. Sci. Technol.* **2010**, 44, 426-431.
34. Qiao, S.; Chen, J.; Li, J.; Qu, Z.; Liu, P.; Yan, N.; Jia, J. Adsorption and Catalytic Oxidation of Gaseous Elemental Mercury in Flue Gas over MnO<sub>x</sub>/Alumina. *Industrial & Engineering Chemistry Research*. **2009**, 48, 3317-3322.
35. Takenami, J.; Uddin, M.; Sasoka, E.; Shioya, Y.; Takase, T. Removal of elemental mercury from dry methane gas with manganese oxides. *World Academy of Science, Engineering and Technology*, **2009**, 32, 26-30.
36. Wang, P.; Su, S.; Xiang, J.; Cao, F.; Sun, L.; Hu, S.; Lei, S. Catalytic oxidation of Hg<sup>0</sup> by CuO-MnO<sub>2</sub>-Fe<sub>2</sub>O<sub>3</sub>/gamma-Al<sub>2</sub>O<sub>3</sub> catalyst. *Chemical Engineering Journal*. **2013**, 225, 68-75.
37. Driscoll, C.; Mason, R.; Chan, H.; Jacob, D.; Pirrone, N. Mercury as a Global Pollutant: Sources, Pathways, and Effects. *Environ. Sci. Technol.* **2013**, 47, 4967-4983.
38. Lalonde, J.; Amyot, M.; Kraepiel, A.; Morel, F. Photooxidation of Hg(0) in artificial and natural waters. *Environ. Sci. Technol.* **2001**, 35, 1367-1372.
39. Lalonde, J.; Amyot, M.; Orvoine, J.; Morel, F.; Auclair, J.C.; Ariya, P. Photoinduced oxidation of Hg<sup>0</sup> (aq) in the waters from the St. Lawrence estuary. *Environ. Sci. Technol.* **2004**, 38, 508-514.
40. Guminski, C. Selected properties of simple amalgams. *J. Mater. Sci.* **1989**, 24, 2661-2676.
41. Gaur, J. & Goswami, N. Kinetics of reduction of Mn<sup>2+</sup> at dropping mercury electrode. *Electrochim. Acta* **1967**, 12, 1483-1488.
42. Biester, H.; Gosar, M.; Muller, G. Mercury speciation in tailings of the Idrija mercury mine. *Journal of Geochemical Exploration* **1999**, 65, 195-204.
43. Taube, F.; Pommer, L.; Larsson, T.; Shchukarev, A.; Nordin, A. Soil remediation - Mercury speciation in soil and vapor phase during thermal treatment. *Water Air Soil Pollut.* **2008**, 193, 155-163.
44. Hocsman, A.; Di Nezo, S.; Charlet, L.; Avena, M. On the mechanisms of dissolution of montroydite HgO(s) : Dependence of the dissolution rate on pH, temperature, and stirring rate. *J. Colloid Interface Sci.* **2006**, 297, 696-704.
45. Schroeder, W. H.; Munthe, J. Atmospheric mercury - An overview. *Atmospheric Environment* **1998**, 32, 809-822.
46. Tomyasu, T.; Kono, Y.; Kodamatani, H.; Hidayati, N.; Rahajoe, J. The distribution of mercury around the small-scale gold mining area along the Cikaniki river, Bogar, Indonesia. *Environ. Res.* **2013**, 125, 12-19.
47. Windmüller, Cláudia C.; Durão Jr., Walter A.; de Oliveira, Aline; do Valle, Cláudia M. The redox processes in Hg-contaminated soils from Descoberto (Minas Gerais, Brazil):

- 487 Implications for the mercury cycle. *Ecotoxicology and Environmental Safety* **2015**, 112,  
488 201–211.
- 489 48. Windmoller, Cláudia Carvalhinho; Santos, Regis Costa; Athayde, Maycon; Palmieri,  
490 Helena Eugênia Leonhardt. Distribution and mercury speciation in sediment gold mining  
491 areas of the Iron Quadrangle (MG). *New Chemical* **2007**, 30, 5, 1088–1094.

492

493

**Figure Captions**

Figure 1: Photographs of mercury beads in (a) soil collected from the mercury spill site at the Y-12 facility in Oak Ridge, TN; (b) uncoated bead of  $\text{Hg}(0)_l$ ; (c, d) coated  $\text{Hg}(0)$  beads after reacting with soil in the laboratory. (e) SEM image of a  $\text{Hg}(0)_l$  bead protruding from a crack in the soil (a), showing a distinct solid phase coating which is likely  $\text{HgO}$ .

Figure 2: (a) SEM images of a mercury bead isolated from contaminated soil (see Fig. 1a) showing distinct Hg associated crystals and clay particles, and (b) a higher resolution image of Hg-containing crystals on the surface of the mercury bead. (c) SEM image and (d) energy dispersive x-ray spectra of pure  $\text{Hg}(0)_l$  (magenta) and a crystal on the surface of the bead (black). The presence of both oxygen ( $\sim 0.5$  keV) and Hg ( $\sim 2.2$  keV) in the crystal, compared with only Hg with no oxygen in the  $\text{Hg}(0)_l$  indicates that the orthorhombic crystal resembles the typical  $\text{HgO}$  mineral montroydite.

Figure 3: Mercury release over time from beads of  $\text{Hg}(0)_l$  placed in deionized water: open symbols are measurements of the dissolved  $\text{Hg}(0)_g$  and filled symbols are the oxidized  $\text{Hg(II)}$  in water. Although dissolved  $\text{Hg}(0)_g$  followed a similar trend,  $\text{Hg}(0)_l$  beads removed from soil (Figure 1a) released a greater amount of oxidized mercury (blue) than did a pure bead (red). The data for the soil Hg beads are presented as the average and standard deviation of the two beads.

Figure 4: Oxidized  $\text{Hg(II)}$  released into water from both treated and untreated  $\text{Hg}(0)_l$  beads measured over time following addition of the water. Bead treatments are summarized in Table 1.

Error bars represent standard deviation of multiple replicate experiments.  $\text{Hg}(0)_1$  reaction time with the solid phase is given for each treatment. The pure bead was not reacted with any solid phase so no reaction time is noted. The reaction time of the  $\text{Hg}(0)_1$  in the in-situ soil sample is not known. The major spills of  $\text{Hg}(0)_1$  at the Y-12 facility occurred between 1950-1953 so this  $\text{Hg}(0)_1$  has likely been reacting with the soil for decades. All experiments were conducted in air except the one labeled with  $\text{N}_2$  was conducted in an  $\text{N}_2$  atmosphere. The samples are grouped as controls (grey),  $\text{Hg}(0)_1$  collected from soil (red), laboratory reacted  $\text{Hg}(0)_1$  in a soil composite (green), and  $\text{Hg}(0)_1$  reacted with manganese oxides (blue), and other solids (yellow).

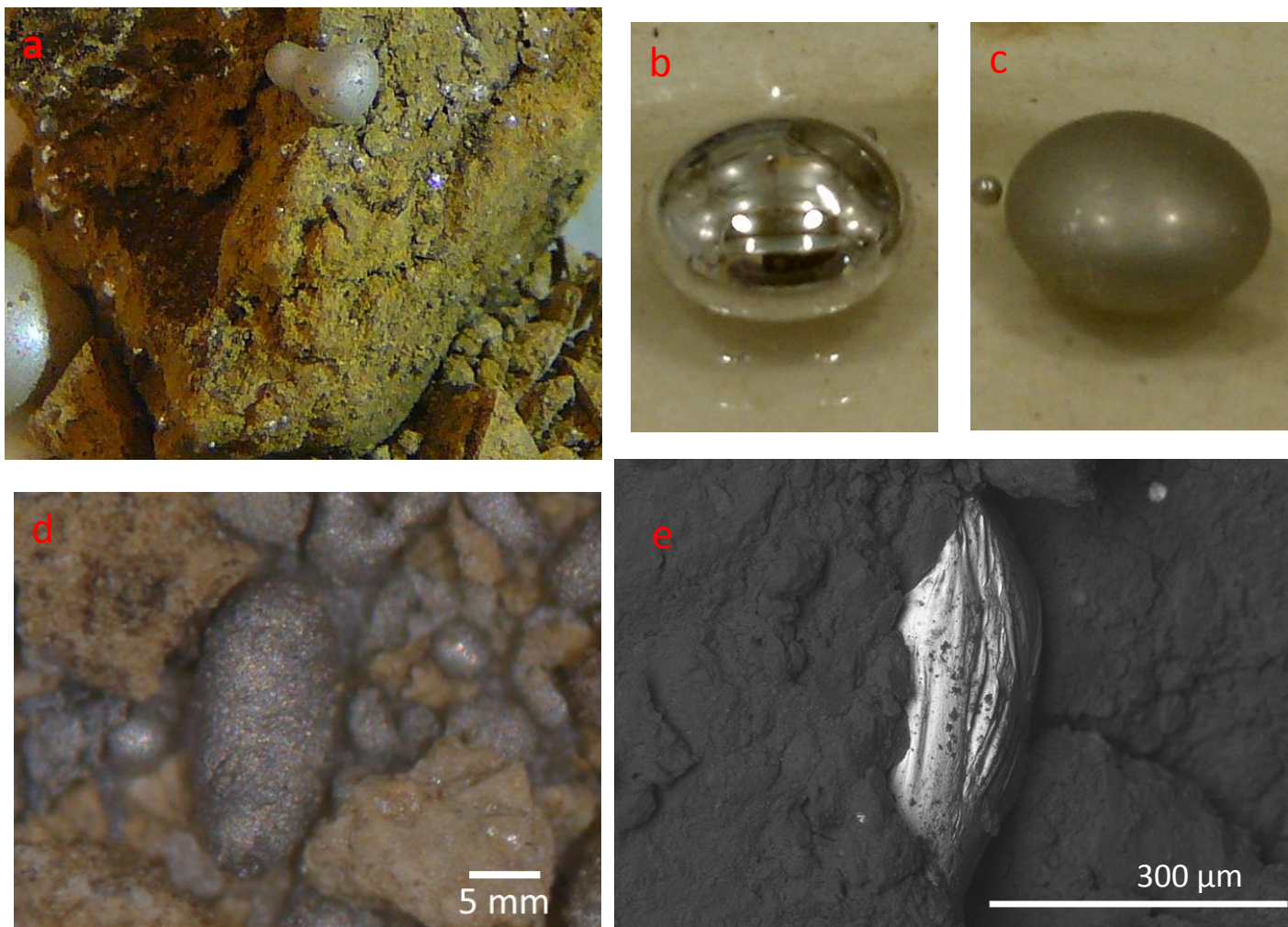


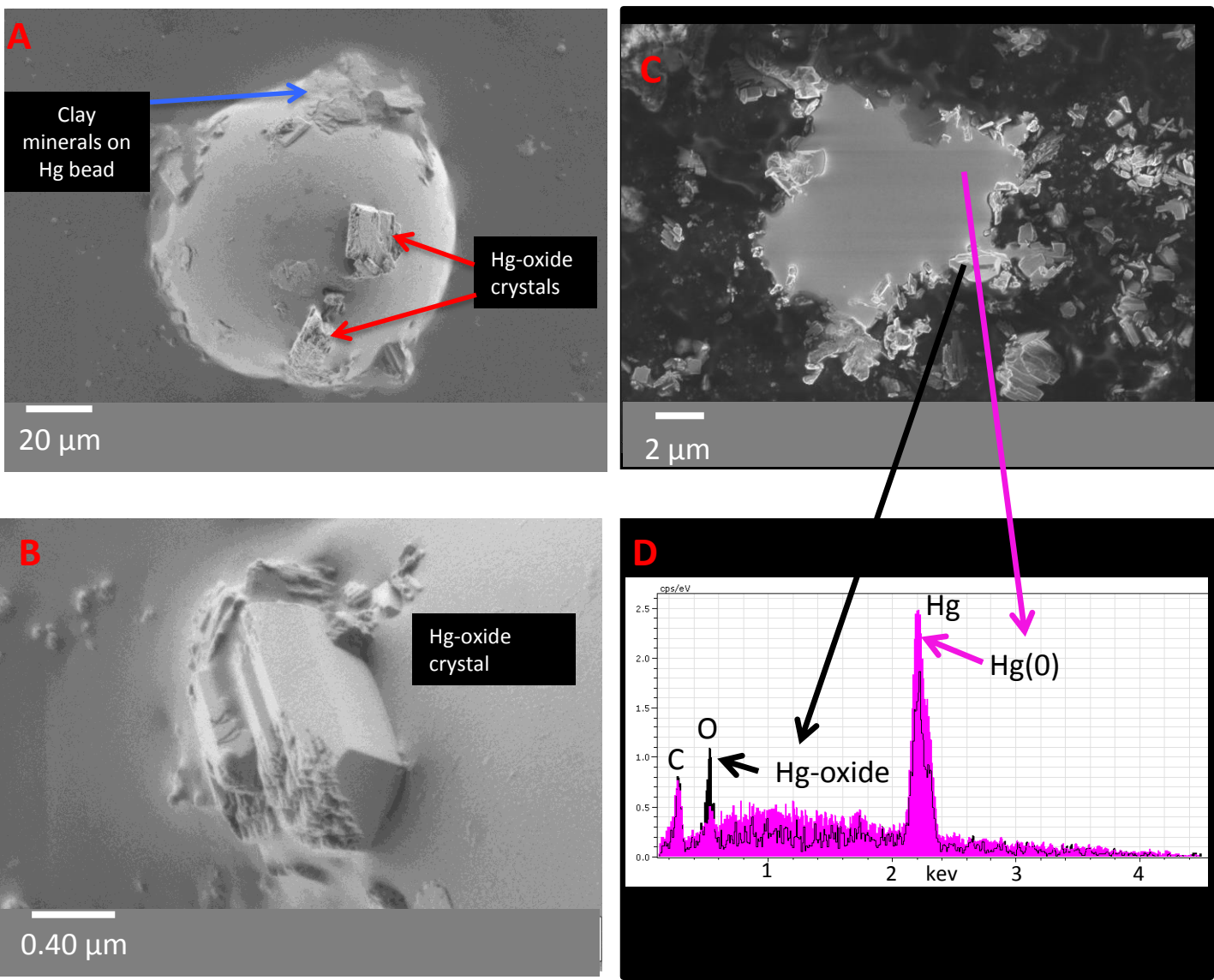
Table 1: Laboratory treatments used to examine the formation of HgO on Hg(0)<sub>l</sub> beads. Hg(0)<sub>l</sub> was incubated in air or with a solid phase.

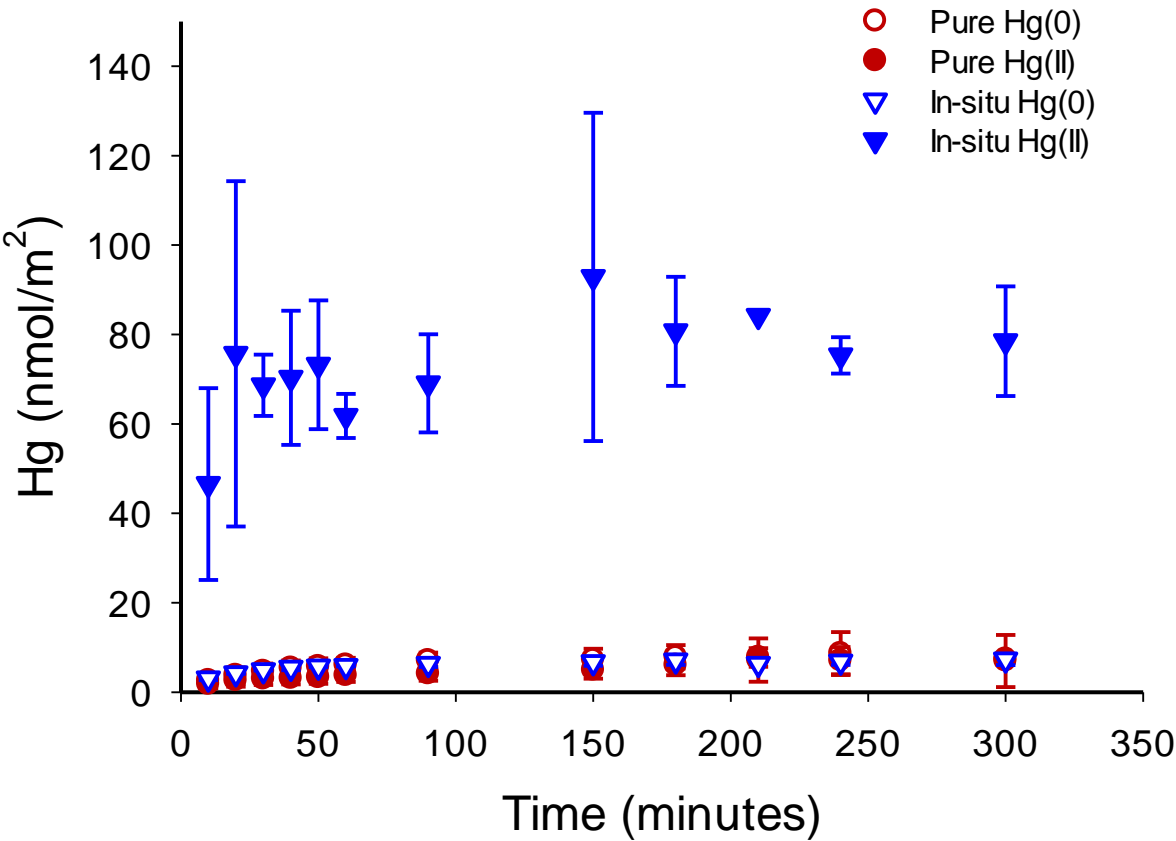
Treatment	Abbreviation	Solid Phase Description	Reaction time
Pure Hg(0) <sub>l</sub>	Pure Hg(0) <sub>l</sub>	No solid, Hg(0) <sub>l</sub> stored under ambient lab air	8-10 days
In-situ soil	In-Situ	Hg(0) <sub>l</sub> removed from a soil core sample collected at the Y-12 facility in Oak Ridge, TN	years
Composite soil, air	Comp, air	Soil composite from soil collected from the Y-12 facility that did not contain Hg(0) <sub>l</sub> . Incubation occurred under ambient lab air.	10, 30 and 157 days
Composite soil, N <sub>2</sub>	Comp, N <sub>2</sub>	Soil composite from soil collected from the Y-12 facility that did not contain Hg(0) <sub>l</sub> . The soil was stored in a anaerobic glove bag prior to the experiment and the incubation occurred under N <sub>2</sub> .	8 days
Manganese (III) oxide	Mn <sub>2</sub> O <sub>3</sub>	Bixbyite; contains 2.4% hausmannite (Mn <sub>3</sub> O <sub>4</sub> )	10 and 120 days
Manganese (III) oxide; dried	Mn <sub>2</sub> O <sub>3</sub> ; dried	Bixbyite; contains 2.4% hausmannite (Mn <sub>3</sub> O <sub>4</sub> ), dried at 105 °C and stored in a N <sub>2</sub> flushed glove bag containing a dessicant	10 days
Manganese (IV) dioxide	MnO <sub>2</sub>	pyrolusite	8 days
Iron oxide	Fe <sub>2</sub> O <sub>3</sub>	hematite	8 days
Quartz sand	sand	acid washed sand (< 150 μm)	8 days
Kaolinite	clay	KGA-2 (kaolinite) CMS** clay reference material	10 days
Soil control	Soil control	Hg(0) <sub>l</sub> and composite soil added to aqueous reaction vessel simultaneously, no solid phase reaction between Hg(0) <sub>l</sub> and soil	0 days

\*The Hg(0)<sub>l</sub> used for all experiments were acid washed Hg(0)<sub>l</sub>, except the in-situ sample which were Hg(0)<sub>l</sub> beads removed from *in situ* soils collected at the Y-12 facility

\*\*Clay Minerals Society







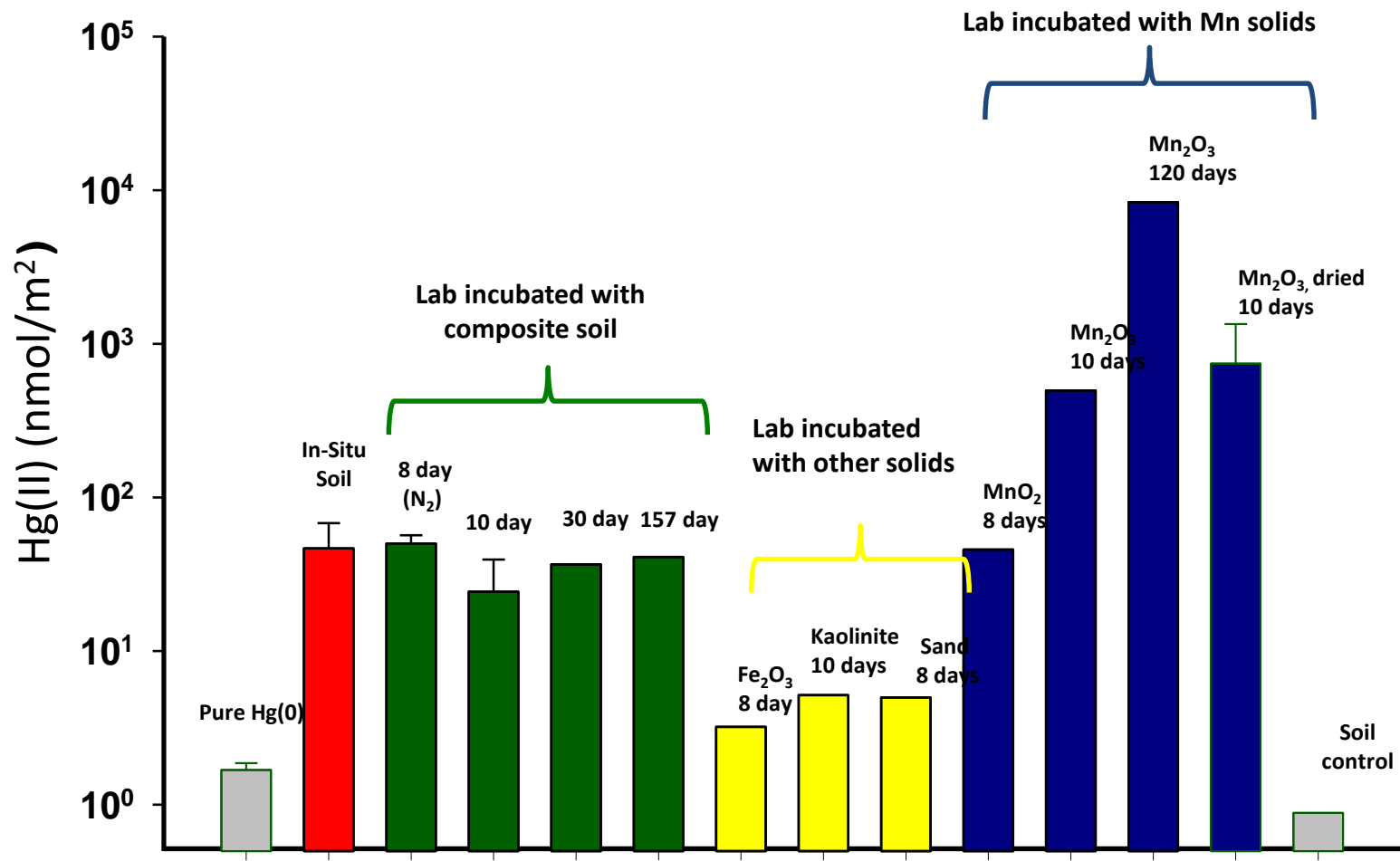


Figure 4

## TOC ART

